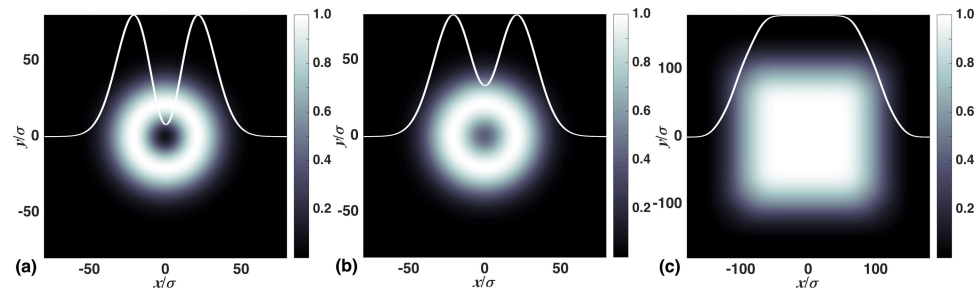


Electromagnetic sinc Schell-Model Vortex Beams

Volume 11, Number 1, February 2019

Zhangrong Mei
Yuyan Wang
Yonghua Mao



DOI: 10.1109/JPHOT.2018.2885012
1943-0655 © 2018 IEEE

Electromagnetic sinc Schell-Model Vortex Beams

Zhangrong Mei^{1,2} Yuyan Wang,^{1,3} and Yonghua Mao¹

¹Department of Physics, Huzhou University, Huzhou 313000, China

²Qizheng School, Huzhou Teachers College, Huzhou 313000, China

³Department of Physics, Zhejiang University of Technology, Hangzhou 310014, China

DOI:10.1109/JPHOT.2018.2885012

1943-0655 © 2018 IEEE. Translations and content mining are permitted for academic research only.

Personal use is also permitted, but republication/redistribution requires IEEE permission.

See http://www.ieee.org/publications_standards/publications/rights/index.html for more information.

Manuscript received October 12, 2018; revised November 27, 2018; accepted December 1, 2018. Date of publication December 4, 2018; date of current version December 28, 2018. This work was supported in part by the Zhejiang Provincial Natural Science Foundation of China under Grant LY16F050007 and in part by the National Natural Science Foundation of China under Grant 11247004 and 11847315. Corresponding author: Zhangrong Mei (e-mail: meizr@zjhu.edu.cn).

Abstract: We introduce a new class of electromagnetic Schell-model source in which the cross-spectral density matrix possesses a sinc correlation function and a separable phase. The far-field radiation properties for the electromagnetic sinc Schell-model vortex beams generated by such source are investigated. It is shown that the far-field distributions of all statistical characteristics of such a beam possess vortex structure, depending on the topological charge and the correlation length of the source field.

Index Terms: Coherence, electromagnetic vortex beams, polarization.

1. Introduction

Optical beams carrying a helical phase structure around the axis with the phase singularity on the axis, known as optical vortices [1], have become the focus of many theoretical investigations and have found applications in optical tweezers [2], micromanipulation [3], optical communications [4] and quantum information processes [5]. The introduction by Gori and co-workers of a phase term with helicoidal structure in the two-point correlation function of an optical field was a milestone for the study of the coherence properties of optical vortices [6]. Since then, a variety of classes of partially coherent beams carefully constructed to carry optical vortex modes have been constructed theoretically and demonstrated experimentally [7]–[12]. However, these related studies have treated the vortex field as a scalar field, and neglected their polarization properties which arise from the vector nature of the electromagnetic field.

A treatment using the cross-spectral density (CSD) matrix provides a unified approach to determine changes of spectral density, polarization and coherence properties of stochastic electromagnetic beams [13], [14]. The electromagnetic Gaussian Schell-model beam is a stochastic electromagnetic beam with the classical analytical model [15]–[18]. Electromagnetic vortex beams cannot be modeled at will because there is rigorous constrain on its cross-spectral density matrix which should fulfill the definiteness property. To date, the studies on the electromagnetic vortex beam are restricted to a model of which the degree of coherence is Gaussian [19]–[21]. The superposition rule [22] for CSD matrices played a significant role in recent studies of stochastic electromagnetic beams with non-Gaussian second-order correlations, such as electromagnetic cos-Gaussian Schell-model beams [23], electromagnetic non-uniformly correlated beams [24], electromagnetic

sinc Schell-model beams [25]. However, the CSD matrices of these stochastic electromagnetic model beams do not possess a phase factor.

The purpose of the present paper is to introduce a new class of stochastic electromagnetic source with a sinc correlation function and a topological phase, and to study the far-field statistical characteristics of beams generated by such source, including intensity, degree of polarization and degree of coherence. In Section 2 presented is the theoretical formulation, where the electromagnetic sinc Schell-model vortex sources are described in the framework of the so-called cross-spectral density matrix. Numerical calculation results and discussion for the far-field statistical properties of the beams generated by such sources are given in Section 3. Finally, the main conclusions are summarized in Section 4.

2. Modeling of CSD Matrix of EMSSM Vortex Sources

The second-order correlation properties of a statistically stationary electromagnetic source at two points ρ'_1 and ρ'_2 may be described by the 2×2 cross-spectral density (CSD) matrix [13]

$$W^{(0)}(\rho'_1, \rho'_2; \omega) \equiv \left[W_{ij}^{(0)}(\rho'_1, \rho'_2; \omega) \right] = \left[\langle E_i^{(0)*}(\rho'_1; \omega) E_j^{(0)}(\rho'_2; \omega) \rangle \right], \quad (i, j = x, y), \quad (1)$$

where $E_i^{(0)}$ and $E_j^{(0)}$ are the mutually orthogonal electric field components in the source plane, the angular bracket denotes the ensemble average over source plane. ρ' is the two-dimensional position vector in the source plane, with polar and Cartesian coordinates of ρ' being (ρ', ϕ') and (x', y') , respectively. In what follows the angular frequency ω depending on all the quantities of interest will be omitted but implied.

For a stochastic electromagnetic vortex beam, the j th component of the complex electric field in the initial transverse plane may be represented as

$$E_j(\rho') = A_j(\rho'/\sigma)^l \exp(-\rho'^2/\sigma^2) \exp(-il\phi') \exp(i\beta_j), \quad (2)$$

where A_j and σ are the maximum source amplitude and the transverse beam width, l is the topological charge, and β_j is the beam phase which may have random statistics in spatial domain. For the sake of computational convenience we assume the statistical distribution of β_j in the source plane corresponds to a Schell-model correlator:

$$C_{ij}^{(0)}(\rho'_1, \rho'_2) = C_{ij}^{(0)}(|\rho'_1 - \rho'_2|). \quad (3)$$

The explicit form of the CSD matrix elements may be expressed by insertion of Eq. (2) into Eq. (1):

$$W_{ij}^{(0)}(\rho'_1, \rho'_2) = A_i A_j (\rho'_1 \rho'_2 / \sigma^2)^l \exp[-(\rho'^2_1 + \rho'^2_2) / \sigma^2] C_{ij}^{(0)}(|\rho'_1 - \rho'_2|) \exp[i l(\phi'_1 - \phi'_2)]. \quad (4)$$

The degree of coherence $C_{ij}^{(0)}(|\rho'_1 - \rho'_2|)$ can employ a variety of proper functions for different coherent distributions in the source field, such as the electromagnetic Gaussian Schell-model source. But the correlation function for optical fields cannot be chosen at will because of the non-negative definiteness constraints [13].

In order to satisfy the nonnegative definiteness property for CSD matrices to be physically realizable, it suffices to have representation of the form [22]

$$W_{ij}^{(0)}(\rho'_1, \rho'_2) = \int p_{ij}(\mathbf{v}) H_i^*(\rho'_1, \mathbf{v}) H_j(\rho'_2, \mathbf{v}) d^2 v. \quad (5)$$

Here, $p_{ij}(\mathbf{v})$ are the elements of the 2×2 weight matrix $\hat{\rho}(\mathbf{v})$, $H_j(\rho', \mathbf{v})$ is an arbitrary kernel which can has plenty of choice and each choice is likely to lead to distinct classes of CSD matrices. The classic Schell-model type can be obtained by assigning to function $H_j(\rho', \mathbf{v})$ a Fourier-like structure. More explicitly, we let

$$H_j(\rho', \mathbf{v}) = F_j(\rho') \exp(-2\pi i \mathbf{v} \cdot \rho'), \quad (6)$$

where F_j is a possible complex profile function. In previous studies, the function F_j was usually set as a real function of Gaussian type, and the models of the electromagnetic stochastic beam were constructed without having phase structure.

To obtain stochastic electromagnetic vortex fields, we set a complex profile function with the phase dependence for the function F_j :

$$F_j(\rho') = A_j(\rho'/\sigma)^l \exp(-\rho'^2/\sigma^2) \exp(-il\phi'). \quad (7)$$

On substituting from Eq. (7) into Eq. (6), then into Eq. (5), the CSD matrix elements takes on the form

$$W_{ij}^{(0)}(\rho'_1, \rho'_2) = A_i A_j (\rho'_1 \rho'_2 / \sigma^2)^l \exp[-(\rho'^2_1 + \rho'^2_2) / \sigma^2] P_{ij}(|\rho'_1 - \rho'_2|) \exp[i l(\phi'_1 - \phi'_2)], \quad (8)$$

where $P_{ij}(|\rho'_1 - \rho'_2|) = \mathcal{F}\{p_{ij}(v)\}$ is the Fourier transform of the function p_{ij} .

On comparing Eq. (4) with Eq. (8), the source degree of coherence takes on the form

$$C_{ij}^{(0)}(|\rho'_1 - \rho'_2|) = \int p_{ij}(v) \exp[i v \cdot (\rho'_1 - \rho'_2)] d^2 v. \quad (9)$$

Hence, a whole class of electromagnetic Schell-model beams with the phase dependence can be obtained by choosing a suitable weight function $p_{ij}(v)$. For example,

$$p_{ij}(v) = \pi B_{ij} \delta_{ij}^2 \exp(-\pi^2 \delta_{ij}^2 v^2), \quad (10)$$

where δ_{ij} are the positive, real constants, and B_{ij} are the correlation coefficient which follows that $B_{ii} = 1$ and $|B_{xy}| = |B_{yx}| \leq 1$. On substituting Eq. (10) into Eq. (8), the following form is obtained:

$$\begin{aligned} W_{ij}^{(0)}(\rho'_1, \rho'_2) &= A_i A_j B_{ij} (\rho'_1 \rho'_2 / \sigma^2)^l \exp[-(\rho'^2_1 + \rho'^2_2) / \sigma^2] \exp[-(x'_2 - x'_1)^2 / \delta_{ij}^2] \\ &\quad \exp[-(y'_2 - y'_1)^2 / \delta_{ij}^2] \exp[i l(\phi'_1 - \phi'_2)]. \end{aligned} \quad (11)$$

Eq. (11) is the CSD matrix elements of electromagnetic Gaussian Schell-model vortex beams.

We shall now consider a new class of electromagnetic vortex beam by considering the following expressions for the weight function $p_{ij}(v)$:

$$p_{ij}(v) = B_{ij} \delta_{ij}^2 \text{rect}(\delta_{ij} v_x) \text{rect}(\delta_{ij} v_y), \quad (12)$$

where $\text{rect}(\cdot)$ is the rectangular function. On inserting Eq. (12) into Eq. (8), the following form is obtained for the CSD matrix elements:

$$\begin{aligned} W_{ij}^{(0)}(\rho'_1, \rho'_2) &= A_i A_j B_{ij} (\rho'_1 \rho'_2 / \sigma^2)^l \exp[-(\rho'^2_1 + \rho'^2_2) / \sigma^2] \text{sinc}[(x'_2 - x'_1) / \delta_{ij}] \text{sinc}[(y'_2 - y'_1) / \delta_{ij}] \\ &\quad \exp[i l(\phi'_1 - \phi'_2)], \end{aligned} \quad (13)$$

which may be called electromagnetic sinc Schell-model (EMSSM) vortex light sources.

3. The Far-Field Radiation Properties Generated by the EMSSM Vortex Light Sources

The elements of the CSD matrix of such source across a transverse plane at distance z can be obtained, under paraxial approximation, by means of the following propagation law [13]

$$W_{ij}(\rho_1, \rho_2) = (\lambda z)^{-2} \iint W_{ij}^{(0)}(\rho'_1, \rho'_2) \exp\left\{-(ik/2z)[(\rho_1 - \rho'_1)^2 - (\rho_2 - \rho'_2)^2]\right\} d^2 \rho'_1 d^2 \rho'_2, \quad (14)$$

where λ is the wavelength, ρ_1 and ρ_2 are transverse position vectors.

After substituting Eq. (13) into Eq. (14), we obtain

$$W_{ij}(\rho_1, \rho_2) = (\lambda z \sigma^l)^{-2} A_i A_j B_{ij} \exp[-(ik/2z)(\rho_1^2 - \rho_2^2)] \iint K_x K_y (x'_1 - iy'_1)^l (x'_2 + iy'_2)^l d^2 \rho'_1 d^2 \rho'_2, \quad (15)$$

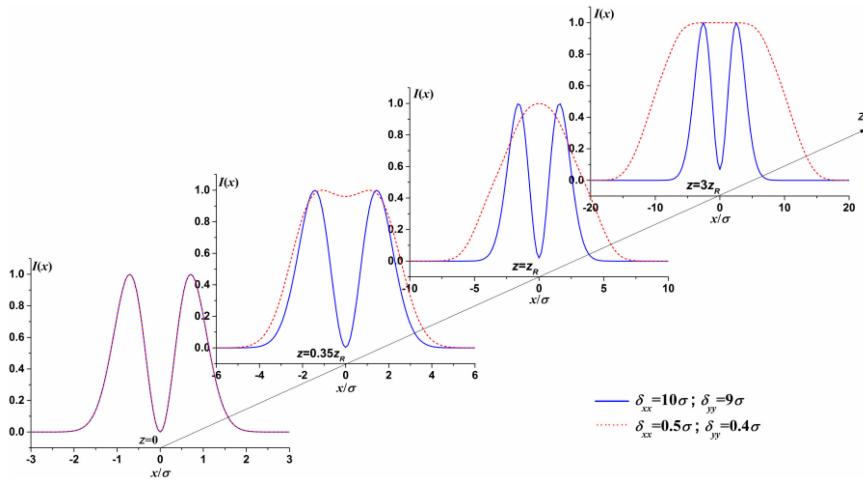


Fig. 1. The evolution of the normalized intensity of the EM SSM vortex beams with topological charge $|l| = 1$, $A_x = A_y = 1$ for different coherence length.

where

$$K_t = \exp \left[-(t_1'^2 + t_2'^2)/\sigma^2 - ik(t_1'^2 - 2t_1t_1' - t_2'^2 + 2t_2t_2')/(2z) \right] \operatorname{sinc} \left[(t_2' - t_1')/\delta_{ij} \right], \quad t = x, y. \quad (16)$$

Numerical integration of Eq. (15) allows us to visualize the statistical properties in any propagating plane, including the intensity distribution $I(\rho)$, the degree of polarization $P(\rho)$ and the degree of coherence $\mu(\rho_1, \rho_2)$, which are respectively given by [13]

$$I(\rho) = \operatorname{Tr} \hat{W}(\rho, \rho), \quad (17)$$

$$P(\rho) = \sqrt{1 - 4 \operatorname{Det} \hat{W}(\rho, \rho) / [\operatorname{Tr} \hat{W}(\rho, \rho)]^2}, \quad (18)$$

$$\mu(\rho_1, \rho_2) = \operatorname{Tr} \hat{W}(\rho_1, \rho_2) / \sqrt{\operatorname{Tr} \hat{W}(\rho_1, \rho_1) \cdot \operatorname{Tr} \hat{W}(\rho_2, \rho_2)}. \quad (19)$$

The four-dimensional integrate of Eq. (15) is generally memory intensive. By expanding the binomial terms in Eq. (15), it can be separated into two-folder integrals:

$$W_{ij}(\rho_1, \rho_2) = \frac{A_i A_j B_{ij}}{(\lambda z \sigma^l)^2} \exp \left[-(ik/2z)(\rho_1^2 - \rho_2^2) \right] \sum_{n=0}^l C_i^n C_j^m \iint K_x x_1'^n x_2'^m dx'_1 dx'_2 \iint K_y (-iy'_1)^{l-n} (iy'_2)^{l-m} dy'_1 dy'_2, \quad (20)$$

where C_i^n and C_j^m stand for binomial coefficients. In the calculation throughout the paper, the following parameters of source are selected: $\sigma = 1$ mm, $\lambda = 632.8$ nm and the far-field plane is set at $z = 30z_R$, where $z_R = k\sigma^2/2$ is the Rayleigh length.

Firstly, in order to have a general image to propagation characteristics of the EM SSM vortex beams, we plot the intensity distribution in Fig. 1 to show their evolving properties for different values of the coherence length. It is evident from the figure that for a high correlation length, the vortex core remains stable on propagation, this is similar to the other vortex beams [10], [19]. And for a low correlation length, the intensity of the dark core will increase with the increase of propagation distance, forming a flat-top profile in the far field, this is similar to the EM SSM without a topological phase [25], the far-field intensity distribution depends on the spatial Fourier transform of the degree of coherence of light across the source and is independent of the shape of the source. The results show that, just as other most Schell-model vortex beams, the vortex structure of such beams will gradually disappear on propagation, and the distance from source field to lose their vortex structure

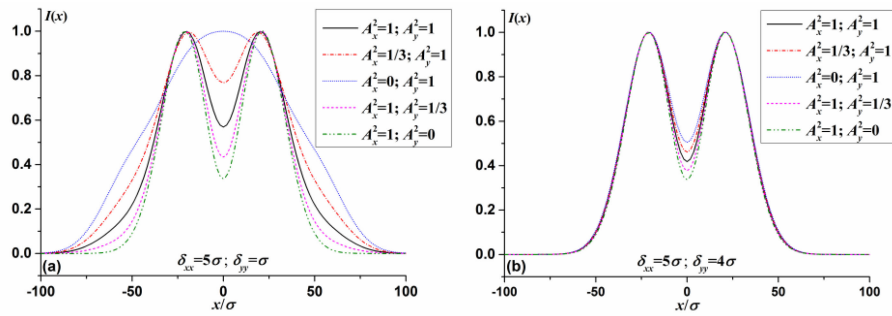


Fig. 2. Normalized far-field intensity of the EM SSM vortex beams for different degree of polarization in the source plane.

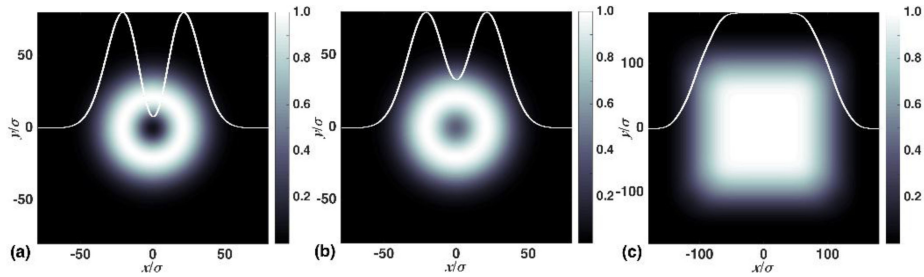


Fig. 3. Normalized intensity of the EM SSM vortex beams in the far zone of sources with topological charge $l=1$ for different coherence length. (a) $\delta_{xx} = 10\sigma$, $\delta_{yy} = 9\sigma$; (b) $\delta_{xx} = 5\sigma$, $\delta_{yy} = 4\sigma$; (c) $\delta_{xx} = 0.5\sigma$, $\delta_{yy} = 0.4\sigma$.

depends on the coherence of the source field. Certainly, not all vortex beams are like this. There are also some partially coherent vortex beams with special coherence characteristics that maintain their vortex structure on propagation [26].

In Fig. 2, we investigate the intensity distribution of the EM SSM vortex beams with topological charge $l=1$ and $B_{xy}=0$ in the far-field plane for different degree of polarization in the source plane. The degree of polarization is selected as $P^{(0)}=0$ ($A_x^2=A_y^2=1$), $P^{(0)}=0.5$ ($A_x^2=1/3$; $A_y^2=1$ or $A_x^2=1$; $A_y^2=1/3$), $P^{(0)}=1$ ($A_x^2=0$; $A_y^2=1$ or $A_x^2=1$; $A_y^2=0$). It can be seen from the figure that the far-field intensity distribution is greatly influenced by the degree of polarization of the source field when the difference between δ_{xx} and δ_{yy} is large, as shown in Fig. 2(a). When δ_{xx} and δ_{yy} are relatively close, the intensity is less affected by the degree of polarization, and the effect is mainly concentrated in the vortex core, as shown in Fig. 2(b).

The far-field intensity, $I(\rho)$, is shown in Fig. 3 for different values of the coherence length. It is evident from Fig. 3 that high coherence of source produces a dark vortex core, its intensity increases and the circularly symmetric profile gradually transforms into a rectangular distribution with the decrease of the coherence length, and finally approaches a rectangular flat-top profile. The corresponding degree of polarization also gradually converts from a circular symmetry to a rectangular distribution with the decrease of the coherence length of source, as shown in Fig. 4. For the high coherence case, the transverse distribution of the degree of polarization also presents a vortex distribution, but the center has a small hump which rises with the decrease of the coherence length. For the low coherence case, Fig. 4(c) shows the formation of a flat rectangular region with uniform degree of polarization in the transverse beam cross-sections. However, unlike the intensity and the degree of polarization, the degree of coherence, calculated by the cross-correlation function $\mu(\rho) = \text{Tr}\hat{W}(\rho, -\rho)/\sqrt{\text{Tr}\hat{W}(\rho, \rho) \cdot \text{Tr}\hat{W}(-\rho, -\rho)}$, maintains the circular profile with a striking dark ring even for the low coherence case, as shown in Fig. 5. Each dark ring exhibits a phase dislocation that is characterized by a π phase jump across the circular boundary. The radius of the dark ring increases as the coherence of the source field decreases.

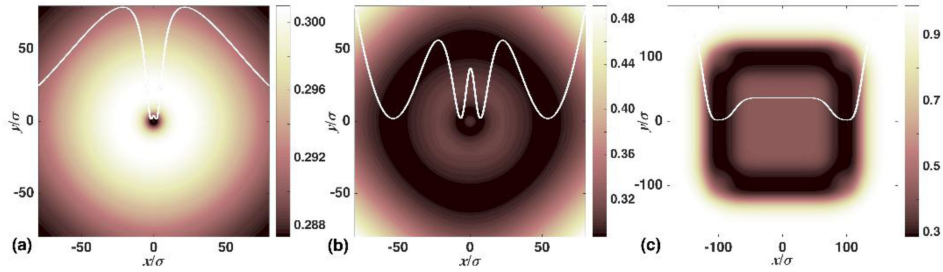


Fig. 4. The degree of polarization of the EM SSM vortex beams in the far zone of sources with parameters as in Fig. 3 except for $B_{xy} = 0.3 \exp(i\pi/3)$ and $\delta_{xy} = \delta_{yx} = \delta_{xx}$.

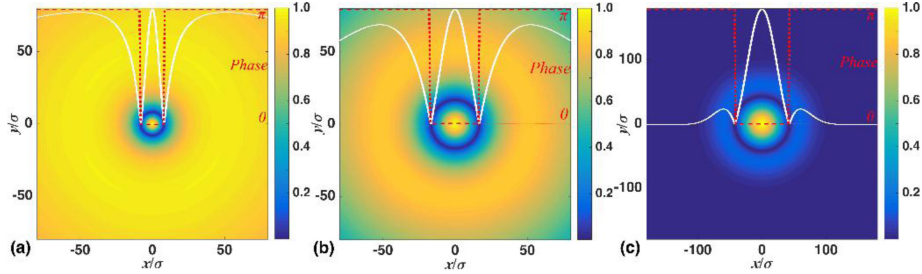


Fig. 5. The degree of coherence corresponding to Fig. 3.

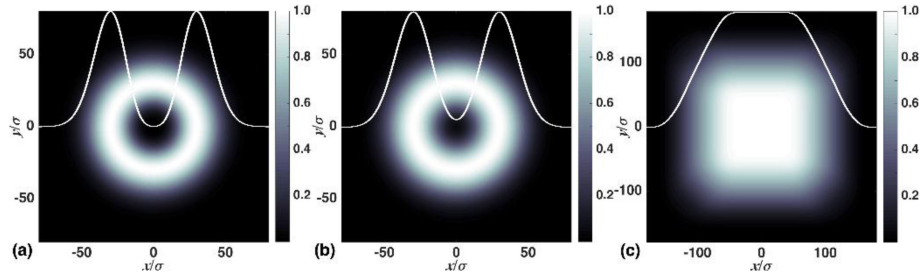


Fig. 6. Far-field intensity as Fig. 3 but for $l = 2$.

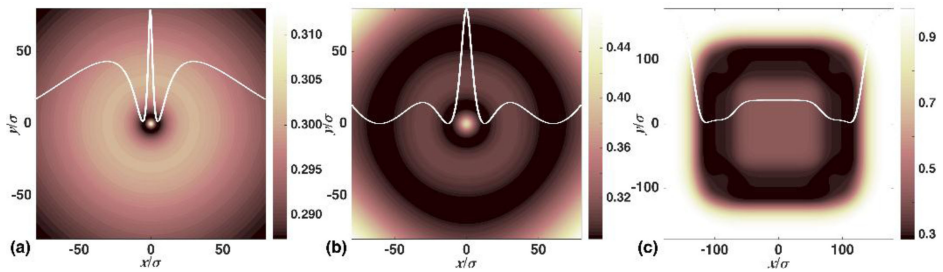
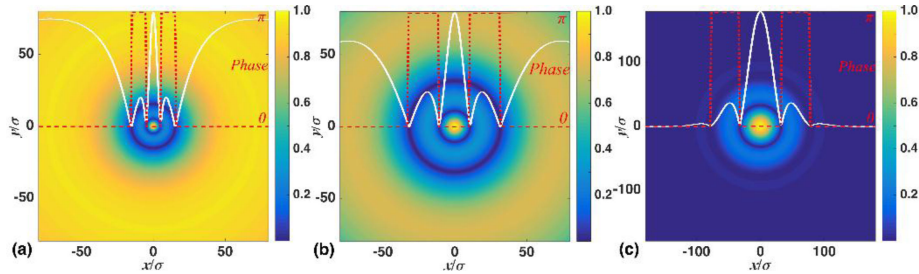


Fig. 7. Far-field degree of polarization as Fig. 4 but for $l = 2$.

Next, let us examine the case where $l = 2$, the intensity, polarization and coherent states are shown in Figs. 6–8, which can be compared with Figs. 3–5 where $l = 1$. It is shown that the intensity profiles are similar to that of $l = 1$, but for the high coherence case the dark core range is larger than $l = 1$ and for low coherence case the flat top region is smaller than $l = 1$. As shown in Fig. 7, the main difference of the polarization distribution between $l = 2$ and $l = 1$ is that the former has a more striking dark ring and the center has a larger hump. In the case of low coherence, both of them have a similar far-field degree of polarization distribution. The main feature of coherent states

Fig. 8. Far-field degree of coherence as Fig. 5 but for $l = 2$.

shown in Fig. 8, compared to the $l = 1$ case, is that two striking dark ring persist as the coherence length is varied, and π phase step exists on the circular boundary of each ring.

4. Summary

Electromagnetic vortex beams cannot be modeled at will because there is rigorous constrain on its cross-spectral density matrix which should fulfill the definiteness property. In this paper, we have proposed a new class of electromagnetic vortex sources with sinc Schell-model correlation on the basis of an application of the general rule for designing cross-spectral density matrices. Furthermore, we demonstrated how the coherence properties and topological charge of the source field affects the statistical characteristics of the far field, including the intensity, the degree of polarization and the degree of coherence, by some numerical examples. The results show that the far-field distributions of all statistical characteristics of such a beam with high coherence possess vortex structure. The intensity vortex has a dark core in the centre of the beam, and the size of the dark core increases with the increase of the topological charge. The polarization vortex has a bright spot at the center, and its height rise with the increase of the topological charge. The coherent distribution in the far field presents ring dislocation, and the number of the rings is equal to the topological charge. In the case of low coherence, the intensity and polarization distributions are similar to those of the general electromagnetic sinc Schell-mode beams without phase factor. But the ring dislocations of the degree of coherence still persist regardless of the size of the source field coherence.

Acknowledgment

The authors wish to thank Dr. Jia Li for a careful reading of this paper and his comments to improve the manuscript.

References

- [1] G. J. Gbur, *Singular Optics*. Boca Raton, FL, USA: CRC Press, 2016.
- [2] W. Lamperska, J. Masajada, S. Drobczyński, and P. Gusin, "Two-laser optical tweezers with a blinking beam," *Opt. Lasers Eng.*, vol. 94, pp. 82–89, 2017.
- [3] J. Ng, Z. Lin, and C. Chan, "Theory of optical trapping by an optical vortex beam," *Phys. Rev. Lett.*, vol. 104, no. 10, 2010, Art. no. 103601.
- [4] J. Wang, "Advances in communications using optical vortices," *Photon. Res.*, vol. 4, no. 5, pp. B14–B28, 2016.
- [5] E. Nagali *et al.*, "Quantum information transfer from spin to orbital angular momentum of photons," *Phys. Rev. Lett.*, vol. 103, no. 1, 2009, Art. no. 013601.
- [6] F. Gori, M. Santarsiero, R. Borghi, and S. Vicalvi, "Partially coherent sources with helicoidal modes," *J. Modern Opt.*, vol. 45, no. 3, pp. 539–554, 1998.
- [7] S. A. Ponomarenko, "A class of partially coherent beams carrying optical vortices," *J. Opt.Soc. Am. A*, vol. 18, no. 1, pp. 150–156, 2001.
- [8] D. M. Palacios, I. D. Maleev, A. S. Marathay, and G. A. Swartzlander, "Spatial correlation singularity of a vortex field," *Phys. Rev. Lett.*, vol. 92, no. 14, 2004, Art. no. 143905.
- [9] R. M.-Herrero, A. Manjavacas, and P. M. Mejías, "Cross-correlation between spiral modes and its influence on the overall spatial characteristics of partially coherent beams," *Opt. Express*, vol. 17, no. 22, pp. 19857–19867, 2009.

- [10] B. Perez-Garcia, A. Yepiz, R. I. Hernandez-Aranda, A. Forbes, and G. A. Swartzlander, "Digital generation of partially coherent vortex beams," *Opt. Lett.*, vol. 41, no. 15, pp. 3471–3474, 2016.
- [11] Z. Mei, "Modeling for partially spatially coherent vortex beams," *IEEE Photon. J.*, vol. 9, no. 5, Oct. 2017, Art. no. 6102306.
- [12] C. S. D. Stahl and G. Gbur, "Partially coherent vortex beams of arbitrary order," *J. Opt. Soc. Am. A*, vol. 34, no. 10, pp. 1793–1799, 2017.
- [13] L. Mandel and E. Wolf, *Optical Coherence and Quantum Optics*, Cambridge, U.K.: Cambridge Univ. Press, 1995.
- [14] O. Korotkova, *Random Light Beams: Theory and Applications*, Boca Raton, FL, USA: CRC Press, 2013.
- [15] F. Gori, "Matrix treatment for partially polarized, partially coherent beams," *Opt. Lett.*, vol. 23, no. 4, pp. 241–243, 1998.
- [16] O. Korotkova and E. Wolf, "Changes in the state of polarization of a random electromagnetic beam on propagation," *Opt. Commun.*, vol. 246, no. 1–3, pp. 35–43, 2005.
- [17] J. Li, M. Zhou, Q. Zhao, and Y. Chen, "Effect of astigmatism on states of polarization of aberrant stochastic electromagnetic beams in turbulent atmosphere," *J. Opt. Soc. Amer. A*, vol. 26, no. 10, pp. 2121–2127, 2009.
- [18] X. Ji, E. Zhang, and B. Lü, "Changes in the spectrum and polarization of polychromatic partially coherent electromagnetic beams in the turbulent atmosphere," *Opt. Commun.*, vol. 275, no. 2, pp. 292–300, 2007.
- [19] Z. Chen and J. Pu, "Stochastic electromagnetic vortex beam and its propagation," *Phy. Lett. A*, vol. 372, no. 15, pp. 2734–2740, 2008.
- [20] S. B. Raghunathan, H. F. Schouten, and T. D. Visser, "Correlation singularities in partially coherent electromagnetic beams," *Opt. Lett.*, vol. 37, no. 20, pp. 4179–4181, 2012.
- [21] M. Luo and D. Zhao, "Determining the topological charge of stochastic electromagnetic vortex beams with the degree of cross-polarization," *Opt. Lett.*, vol. 39, no. 17, pp. 5070–5073, 2014.
- [22] F. Gori, V. Ramirez Sanchez, M. Santarsiero, and T. Shirai, "On genuine cross-spectral density matrices," *J. Opt. A Pure Appl. Opt.*, vol. 11, no. 8, 2009, Art. no. 085706.
- [23] Z. Mei and O. Korotkova, "Electromagnetic cosine-Gaussian Schell-model beams in free space and atmospheric turbulence," *Opt. Express*, vol. 21, no. 22, pp. 27246–27259, 2013.
- [24] Z. Tong and O. Korotkova, "Electromagnetic nonuniformly correlated beams," *J. Opt. Soc. Amer. A*, vol. 29, no. 10, pp. 2154–2158, 2012.
- [25] Z. Mei and Y. Mao, "Electromagnetic sinc Schell-model beams and their statistical properties," *Opt. Express*, vol. 22, no. 19, pp. 22534–22546, 2014.
- [26] G. V. Bogatyryova, C. V. Fel'de, P. V. Polyanskii, S. A. Ponomarenko, M. S. Soskin, and E. Wolf, "Partially coherent vortex beams with a separable phase," *Opt. Lett.*, vol. 28, no. 11, pp. 878–880, 2003.